PNAS RESEARCH ARTICLE | EVOLUTION

Middle Jurassic fossils document an early stage in salamander evolution

Marc E. H. Jones[a,1], Roger B. J. Benson[b], Pavel Skutschas (Павел Скучас)[c], Lucy Hill[a,d], Elsa Panciroli[e,f], Armin D. Schmitt[b], Stig A. Walsh[f], and Susan E. Evans[a]

Edited by Neil Shubin, The University of Chicago, Chicago, IL; received August 3, 2021; accepted April 29, 2022

Salamanders are an important group of living amphibians and model organisms for understanding locomotion, development, regeneration, feeding, and toxicity in tetrapods. However, their origin and early radiation remain poorly understood, with early fossil stem-salamanders so far represented by larval or incompletely known taxa. This poor record also limits understanding of the origin of Lissamphibia (i.e., frogs, salamanders, and caecilians). We report fossils from the Middle Jurassic of Scotland representing almost the entire skeleton of the enigmatic stem-salamander *Marmorerpeton*. We use computed tomography to visualize high-resolution three-dimensional anatomy, describing morphologies that were poorly characterized in early salamanders, including the braincase, scapulocoracoid, and lower jaw. We use these data in the context of a phylogenetic analysis intended to resolve the relationships of early and stem-salamanders, including representation of important outgroups alongside data from high-resolution imaging of extant species. *Marmorerpeton* is united with *Karaurus*, *Kokartus*, and others from the Middle Jurassic–Lower Cretaceous of Asia, providing evidence for an early radiation of robustly built neotenous stem-salamanders. These taxa display morphological specializations similar to the extant cryptobranchid "giant" salamanders. Our analysis also demonstrates stem-group affinities for a larger sample of Jurassic species than previously recognized, highlighting an unappreciated diversity of stem-salamanders and cautioning against the use of single species (e.g., Karaurus) as exemplars for stem-salamander anatomy. These phylogenetic findings, combined with knowledge of the near-complete skeletal anatomy of *Mamorerpeton*, advance our understanding of evolutionary changes on the salamander stem-lineage and provide important data on early salamanders and the origins of Batrachia and Lissamphibia.

evolution | phylogeny | amphibians | Jurassic | salamander

Salamanders comprise 760+ living species and are important components of terrestrial and freshwater ecosystems (1, 2). They are ecologically and developmentally diverse, including burrowers, climbers, cave dwellers and neotenic swimmers, and exhibit great variation in life history and degrees of parental care (3–5). Salamanders are also important as model organisms (6) for investigating development (7–9), regeneration (10, 11), terrestrial locomotion (12), skull shape (13), body shape (14), feeding (3), genome size (15), and toxicity (16). However, their evolutionary origins are poorly understood, and the fossil record of early lissamphibians, including salamanders, is poor. Stem frogs are known from the Early Triassic (17, 18), giving a latest possible date (250 Ma) for the divergence of the frog and salamander stem-lineages. However, aside from *Triassurus* from the Middle/Upper Triassic of Kyrgyzstan (19), which is known from two larval specimens (20), there is little detailed anatomical data for stem salamanders (i.e., stem urodeles) before the Late Jurassic.

The fossil record of Mesozoic total-group salamanders (Caudata) has increased dramatically in the last 20 years, based predominantly on specimens from the Middle Jurassic–Early Cretaceous of Asia (21–28). To date, most such species have been identified as members of the salamander crown-group (21–24, 27): Urodela. Knowledge of the stem-lineage has lagged behind, impeding understanding of the origin and early diversification of salamanders. Many studies have relied on the likely stem-salamander *Karaurus sharovi* from the Upper Jurassic of Kazakhstan (19), as a solitary outgroup in phylogenetic analysis (*SI Appendix*, Table S1). This species is known from a well-preserved and almost complete skeleton. However, it is partially embedded in rock matrix, limiting understanding of important anatomical regions, especially the braincase and mandible. Furthermore, no taxon is individually representative of an ancestral morphology, or free from independently derived specializations. In this context, additional information on well-preserved stem-salamanders is key to understanding the early evolution of salamanders, and will inform studies of lissamphibian origin(s) more broadly (20).

Significance

Little is known about stem-lineage salamanders, limiting understanding of their early evolution and of the origins of modern amphibian diversity. We report new, three-dimensionally preserved skeletons of the stem-salamander *Marmorerpeton*, from 166 million-year-old rocks in Scotland, documenting many phylogenetically informative anatomical traits. High resolution computed tomography (CT) scans reveal unprecedented three-dimensional anatomical detail, illuminating anatomical changes during early salamander evolution. Phylogenetic analysis provides evidence for an anatomically diverse radiation of early stem salamanders distributed across Eurasia during the Middle Jurassic and Early Cretaceous. Our findings highlight the morphological variety of stem-salamanders, undermining the use of single exemplars (e.g., *Karaurus*; the "*Archaeopteryx*" of salamanders) to represent early evolutionary transitions.

Author contributions: M.E.H.J., R.B.J.B., and S.E.E. designed research; M.E.H.J., R.B.J.B., P.S., and S.E.E. performed research; M.E.H.J., R.B.J.B., L.H., E.P., A.D.S., and S.E.E. analyzed data; M.E.H.J. wrote the paper; R.B.J.B., S.A.W., and S.E.E. contributed new reagents/analytic tools; M.E.H.J. wrote first draft of the manuscript; R.B.J.B., E.P., A.D.S., S.A.W., and S.E.E. contributed to final version of the manuscript; and P.S. contributed to the final version.

The authors declare no competing interest.

This article is a PNAS Direct Submission.

Copyright © 2022 the Author(s). Published by PNAS. This article is distributed under Creative Commons Attribution-NonCommercial-NoDerivatives License 4.0 (CC BY-NC-ND).

[1]To whom correspondence may be addressed. Email: marc.jones@ucl.ac.uk.

This article contains supporting information online at http://www.pnas.org/lookup/suppl/doi:10.1073/pnas.2114100119/-/DCSupplemental.

Published July 11, 2022.

Downloaded from https://www.pnas.org by UCL Library Services on July 25, 2022 from IP address 128.41.35.168.

Various other early stem-salamanders have also been reported, but are relatively poorly known (*SI Appendix*, Table S2). *Triassurus sixtelae* from the Middle/Upper Triassic of Kyrgyzstan was based on a poorly preserved skeletal impression of a single larval specimen (19). However, the recent discovery of a second more complete specimen has confirmed its identification as an early stem-salamander, with implications for the early anatomical divergence of the group (20). *Kokartus honorarius* from the Middle Jurassic of Kyrgyzstan is known from both isolated and associated specimens (26, 29, 30), although none is as complete as the holotype of *Karaurus* (19). *Kokartus* and *Karaurus* are both generally assigned to Karauridae on the shared presence of heavily sculpted skull roofing bones in both genera (20, 29, 31, 32). Other attributed stem-salamanders are known from isolated parts of the axial skeleton, skull, or major limb elements. These include *Marmorerpeton kermacki*, *M. freemani*, and "Salamander A" from the Middle Jurassic of the United Kingdom (33, 34), *Urupia monstrosa* and *Egoria malashichevi* from the Middle Jurassic of Russia (26, 35), and *Kulgeriherpeton ultimum* and an indeterminate stem salamander from the Lower Cretaceous of Russia (25). This material is often well-preserved in three dimensions (25, 36) but is very incomplete. For example, both species of *Marmorerpeton* from the Bathonian of Kirtlington (England) remain largely undescribed except for the atlas, other vertebrae, partial jaws, exoccipitals, a partial vomer, and possibly a humerus (33).

Here, we describe a species of *Marmorerpeton* from the Middle Jurassic (Bathonian) of the Isle of Skye (Scotland), based on high-resolution three-dimensional (3D) imaging of several specimens with little to no crushing. Our specimens include most of the postcranium as well as a nearly complete skull, including the braincase and lower jaws that were previously poorly known in stem-salamanders. We use these data in a comprehensive phylogenetic reassessment of fossil salamander relationships, supported by high-resolution 3D imaging of the anatomy of living salamander species from all major groups. Our results confirm that *Marmorerpeton* is a member of Karauridae (with *Karaurus* and *Kokartus*), which is in turn part of a previously unrecognized clade of Eurasian stem-salamanders. The results also suggest that various Jurassic and Early Cretaceous fossil taxa belong to the salamander stem lineage rather than within the crown-group (Urodela), and demonstrate a complex step-wise character acquisition during early salamander evolution.

Results

Description of the New Material.

Systematic paleontology. Tetrapoda Haworth, 1825; Lissamphibia Haeckel, 1866; Caudata Scopoli, 1777; Karauridae Ivakhnenko, 1978; *Marmorerpeton* Evans, Milner and Mussett, 1988; *Marmorerpeton wakei* sp. nov.

Etymology. *wakei* in honor of the late Professor David Wake for his ground-breaking work on salamanders.

Holotype. NMS (National Museums Scotland, Edinburgh, UK) G.2021.4.3, an associated skeleton that includes a complete atlas, exoccipital, orbitosphenoid, prootic, maxilla, prefrontal, pelvic girdle, femur, terminal phalanx, ribs, and almost complete tail (Figs. 1 and 2). A vertebra of this specimen was figured as *Marmorerpeton*, in (34), under field number "ELGOL.2016.024" (*SI Appendix*, Table S3).

Referred material. Three partial skeletons: NMS G.1992.47.9, NMS G.2021.4.1, and NMS G.2021.4.2, which includes most of the skull (~35 mm long) (Fig. 1; the preserved elements of these specimens are listed in *SI Appendix*, Tables S3–S5; and illustrated as-preserved in *SI Appendix*, Figs. S1–S6); and NMS G.1992.47.13, an ilium. CT scans and 3D models of all four new specimens are provided at MorphoSource (37).

Type locality and horizon. The specimens come from the Bathonian (Middle Jurassic) Kilmaluag Formation on the Straithaird Peninsula north of Elgol and ~1 km south of Cladach a'Ghlinne (34). New specimens were recovered in 2014 (NMS G.2021.4.1), 2016 (NMS G.1992.47.9.2-3; NMS G.2021.4.3) and 2019 (NMS G.2021.4.2). One of these specimens, NMS G.1992.47.9.2-3, is part of a hitherto undescribed specimen that was partially collected by Robert Savage and Michael Waldman in 1971 (NMS G.1992.47.9.1) (38).

Diagnosis. A Middle Jurassic stem-salamander belonging to *Marmorerpeton*, that differs from *Marmorerpeton kermacki* and *M. freemani* in having an atlas with a relatively even distribution of porosity, the absence of elongate grooves on the lateral surfaces, and the absence of a deep central depression on the ventral surface. The atlas of *M. wakei* also has taller ovoid atlantal cotyles unlike the dorso-ventrally shallower elliptical cotyles of *M. freemani* (*SI Appendix*, Part C). *M. wakei* also has an atlas with a posterior width that is 46% of the anterior width (50–57% in *M. kermacki*; 37% in *M. freemani*) (*SI Appendix*, Part C and Fig. S9).

M. wakei is similar to the type species *Marmorerpeton kermacki* in having a premaxilla with a posterior shelf; a dentary with a prominent circular medial symphysis; and an atlas that is longer than wide, lacks spinal nerve foramina, lacks transverse processes, has a flattened and pitted ventral surface, has a small odontoid process (tuberculum interglenoideum) that is perforated by the notochord, and has an elongated lower lip that protrudes relative to the upper lip (Fig. 2 *A–D* and *SI Appendix*, Fig. S57) (33). Based on first-hand comparisons with undescribed material from the type locality (Kirtlington, Oxfordshire, UK), *M. wakei* also resembles *M. kermacki* in having skull bones with broad overlaps and heavy pit-and-ridge sculpture; exoccipitals separate from surrounding bones, and each with a large ventral recess for the parasphenoid and large anterolaterally positioned vagus foramen; a vomer with a gently curved row of at least nine teeth; amphicoelous vertebrae bearing a single unfinished neural spine; circular vertebral cotyles of greater diameter than the neural canal; a scapulocoracoid with a buttress-like glenoid; and a coracoid foramen partly enclosed by bone (*SI Appendix*, Table S7) (33).

M. wakei is known from significantly more complete material than *M. kermacki* or *M. freemani* (*SI Appendix*, Part E), and shares features with *Karaurus* and *Kokartus* such as a prefrontal with a prominent posterolateral process, roofing bones with heavy pit-and-ridge sculpture, and vertebrae with cotyles that have a greater diameter than their neural canal (*SI Appendix*, Table S7). The ventral surface of the dorsal vertebrae may also exhibit a midline depression (*SI Appendix*, Fig. S61) as previously reported for both *Marmorerpeton* and *Kokartus* (30, 33).

Paleoenvironment. The skeletons were deposited in low-salinity lagoons or coastal lakes with input from small rivers (39, 40). The fossil assemblage is diverse, representing actinopterygian and chondrichthyan fishes, amphibians, stem-lepidosaurs, lizards, choristoderes, turtles, archosaurs and mammaliaforms (34).

Skull. We conducted high-resolution computed tomographic (CT) scans of the holotype and referred specimens of *Marmorerpeton wakei* (Figs. 1 and 2; *SI Appendix*, Tables S3–S5). These provide exceptional detail for almost all skull bones, allowing an almost complete digital restoration of the skull morphology after minimal retrodeformation and rescaling of elements

Downloaded from https://www.pnas.org by UCL Library Services on July 25, 2022 from IP address 128.41.35.168.

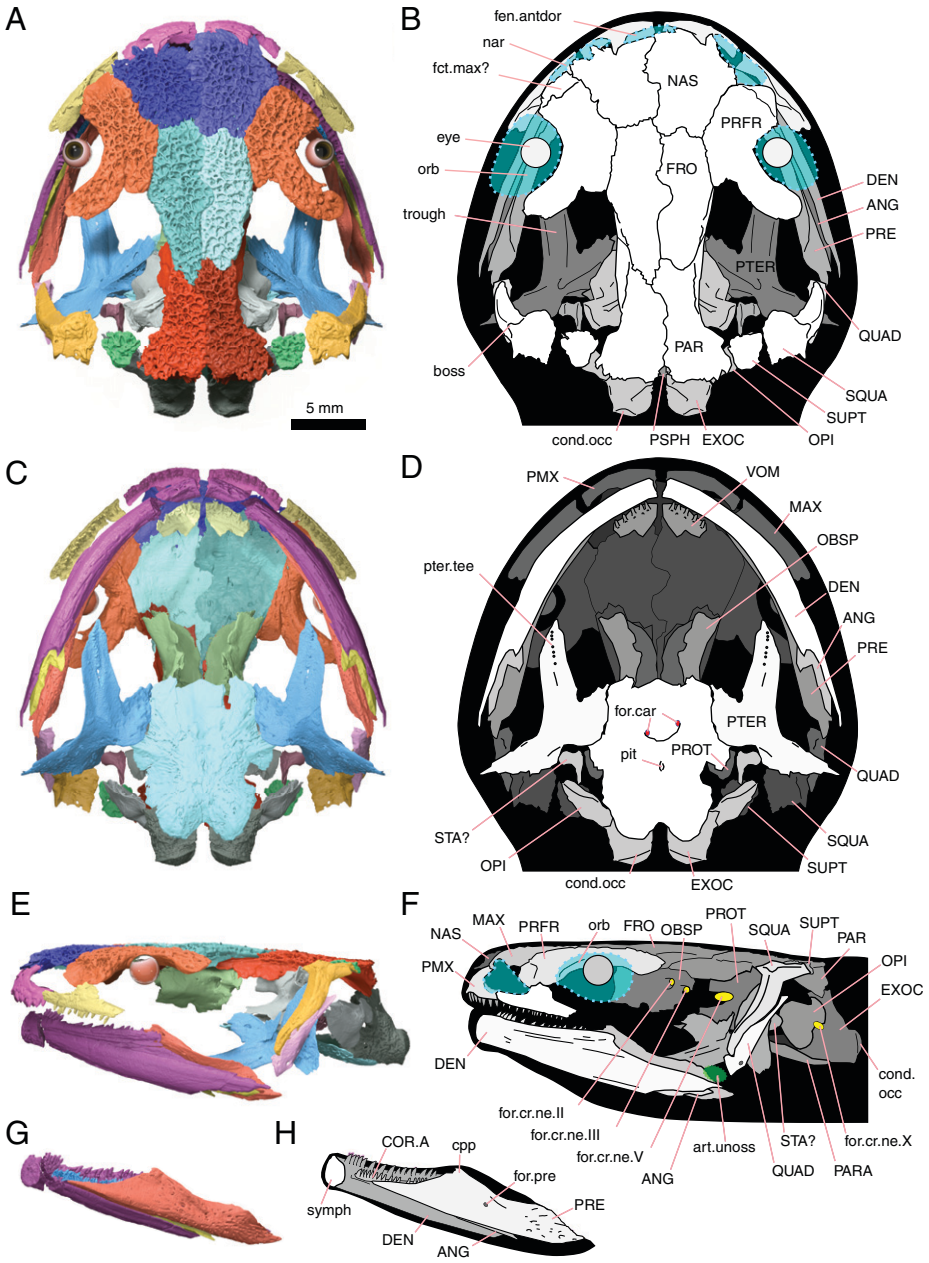

Fig. 1. Reconstruction of cranium and lower jaw of *Marmorerpeton wakei* (based mainly on NMS G.2021.4.2, see *SI Appendix*, Table S9 and Fig. S22 for original preservation conditions). Cranium shown in dorsal (*A* and *B*), ventral (*C* and *D*), and lateral (*E* and *F*) views with lower jaw shown in medial view (*G* and *H*). Please note that the rhomboid element (*SI Appendix*, Fig. S55) and possible branchial denticles (*SI Appendix*, Fig. S56) are not included in the restoration as their identification remains uncertain as discussed in *SI Appendix*, Part E. ANG, angular; art.unoss, hypothesized position of cartilaginous articular surface; cond.occ, occipital condyle; COR.A, coronoid anterior; cpp, coronoid process of the prearticular; DEN, dentary; EXOC, exoccipital; fct.max, facet for the maxilla or lacrimal; fen.antdor, anterodorsal fenestra; for.car, foramina for the internal carotid arteries; for.cr.ne.II, foramen for the optic nerve CN II; for.cr.ne.III, foramen for the oculomotor nerve CN III; for.cr.ne.V, foramen for the trigeminal nerve CN V; for.cr.ne.X, foramen for the jugular vein and vagus nerve CN X; for.pre, prearticular foramen; FRO, frontal; MAX, maxilla; nar, naris; NAS, nasal; OBSP, orbitosphenoid; OPI, opisthotic; orb, orbit; PARA, parasphenoid; PAR, parietal; pit, hypophyseal fossa?; PMX, premaxilla; PRE, prearticular; PROT, prootic; PSPH, parasphenoid; PRFR, prefrontal; PTER, pterygoid; QUAD, quadrate; SQUA, squamosal; STA?, possible stapes; SUPT, supratemporal; symph, symphysis; tee.pter, pterygoid teeth; VOM, vomer.

(Fig. 1 and *SI Appendix*, Part D). The reconstructed cranium primarily based on NMS G.2021.4.2 is longer than it is wide (length = 27 mm; width = 23 mm). However, the prefrontal of NMS G.2021.4.3 is larger and relatively broader; *SI Appendix*, Fig. S33) and suggests a larger and proportionally broader skull (length = 32 mm; width = 33 mm; *SI Appendix*, Fig. S23) similar to the skull proportions of many other batrachians (20, 41). This relatively wider skull in larger individuals more closely approaches the size and proportions of the only known skull of *Karaurus* (19) (length = 40 mm; width = 50 mm) particularly given that postmortem dorsoventral compression has likely exaggerated its width. Nevertheless, *M. wakei* differs from *Karaurus* with respect to relative snout length (~25% of skull length compared to 34%). The ontogenetic increase in relative skull width inferred for *M. wakei* is similar to that reported for other temnospondyls (42, 43).

The skull of *M. wakei* is dorsoventrally shallow, has a broad snout, a narrow skull table, and strut-like squamosals that extended anterolaterally (Fig. 1). All of the major skull roofing elements (including the small supratemporal) bear a heavy pit-and-ridge sculpture similar to karaurids (29) and some possible stem-lissamphibians such as *Apateon* and *Amphibamus* (43).

Downloaded from https://www.pnas.org by UCL Library Services on July 25, 2022 from IP address 128.41.35.168.

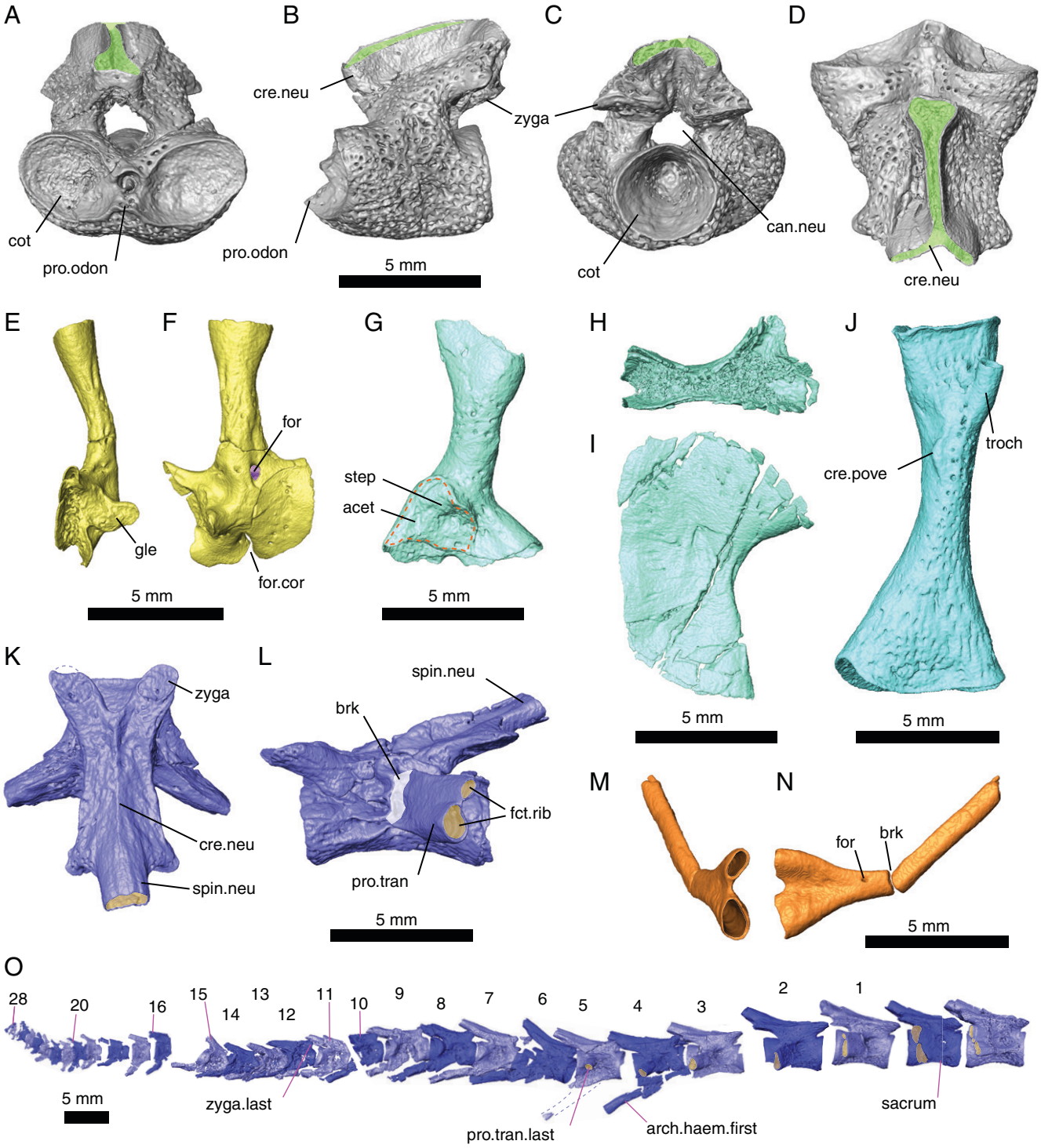

Fig. 2. Postcrania of *Marmorerpeton wakei*: atlas (*A*, *B*, *C*, *D*) in anterior (*A*), left lateral (*B*), caudal (*C*), dorsal (*D*) view; left scapulocoracoid (*E* and *F*) in rostral (*E*) and lateral (*F*) views; left ilium (*G*) in lateral view; left ischium (*H* and *I*) in rostral (*H*) and ventral (*I*) view; left femur in ventral view (*J*); caudal vertebra (*K* and *L*) in dorsal (*K*) and left lateral (*L*) view; rib in proximal (*M*) and rostral view (*N*); near-articulated tail of holotype specimen in right lateral view (*O*) (sacrum and last dorsal reversed). Caudal vertebrae 1–4 represent the caudosacrals as defined elsewhere (27). For specimen numbers, see *SI Appendix*, Table S6. Abbreviations: acet, acetabulum; arch.haem.first, first haemal arch; brk, breakage; cre.pove, posteroventral crest; cre.neu, neural crest; cot, cotyle; for, foramen; gle, glenoid; for.cor, coracoid foramen. arch.haem first, first haemal arch; cres.neu, neural crest; neu.can, neural canal; neu.cre, neural crest; neu.spin, neural spine; odon.pro, odontoid process; pro.tran last, last transverse process; rib.fct, rib facet; spin.neu, neural spin; tr.pro, transverse process; troch, trochanter; zyga, zygapophysis; zyga.last, last zygapophysis.

There is a large orbitotemporal opening, as in most batrachians, although it is interrupted by a prominent posterolateral process of the prefrontal, which probably marks the posteromedial boundary of the orbit, indicating an anterolateral position for the eye (*SI Appendix*, Figs. S31–S33). A similar but less prominent process is present in *Karaurus* (19, 45) and possibly *Kokartus* (29). The eye is also located anterolaterally within the orbitotemporal opening in cryptobranchids (3), which lack any development of a prefrontal process.

The parietals are L-shaped (Fig. 1 *A* and *B*), which is a synapomorphy of Caudata (20). The parietals also have an anterolateral process extending lateral to the frontal (Fig. 1 *E* and *F*),

Downloaded from https://www.pnas.org by UCL Library Services on July 25, 2022 from IP address 128.41.35.168.

a feature that is widespread among crown-salamanders and also present in Mesozoic taxa from the Upper Jurassic of China such as *Beiyanerpeton*, *Qinglongtriton* (21, 24), and *Chunerpeton* (28). The posterior end of the parietal has a ventrolateral shelf facing caudally (Fig. 1 *E* and *F* and *SI Appendix*, Figs. S36–S38) as seen in some modern salamanders (e.g., *Siren* and *Amphiuma*), and also on the postparietals of dissorophoids (46). The frontals and parietals are relatively narrow whereas the nasals are relatively wide, resembling the skull table proportions of hynobiid salamanders. The frontal and parietal also have ventrolateral shelves facing laterally, similar to those in *Karaurus* (19) and *Kokartus* (29), that would have provided sites of origin for the jaw muscles. However, the presence of sculpture on the dorsal surface of these bones suggests that the jaw muscles of *M. wakei* did not extend onto the dorsal surface, therefore differing from most crown-group salamanders (3).

The premaxillae are paired, have a triangular acuminate alary process that slots into the nasal, a short palatal shelf, and each has a row of at least 17 teeth (*SI Appendix*, Figs. S24 and S25). Due to the triangular and asymmetrical alary process, the premaxilla resembles the "type B" premaxilla associated with the *Marmorerpeton* material from Kirtlington (33). The maxilla is incompletely known but has a facial process, short palatal shelf, and spaces to bear at least 21 teeth (*SI Appendix*, Fig. S29). A tall triangular internal process resembles that of the "type C" maxilla associated with the *Marmorerpeton* material from Kirtlington (33). The teeth do not appear to be pedicellate or bicuspid but evaluation of this trait is limited by resolution of the micro CT data. However, teeth referred to *Marmorerpeton* sp. from Kirtlington, United Kingdom, are bicuspid and weakly pedicellate (33). A septomaxilla may be present adjacent to the narial margin of an incomplete maxilla (*SI Appendix*, Fig. S30).

Palate. The vomer is incompletely known but has a row of at least nine teeth along the inferred anterolateral margin (Fig. 1 *C* and *D* and *SI Appendix*, Fig. S44) and is similar to that of cryptobranchid salamanders. The pterygoid has a large posterior process for contact with the quadrate and/or squamosal and a medial shelf for contact with the prootic and parasphenoid (*SI Appendix*, Figs. S45 and S46). It has a single tooth row located on its anterior process (Fig. 1 *C* and *D*) as found in neotenic adults of the amphibamiform *Apateon caducus* (44), Mesozoic salamanders such as *Kokartus*, *Beiyanerpeton*, *Qinglongtriton*, and *Chunerpeton* (21, 24, 28, 29), and larval forms of some modern salamanders (47). The pterygoid has a shallow trough on its dorsal surface (Fig. 1 *A* and *B* and *SI Appendix*, Figs. S44 and S45), a common feature among fossil and extant salamanders (related to the pterygoquadrate cartilage) but absent in Gymnophiona (48). Evidence for an ossified hyoid apparatus has yet to be identified but these structures may have been cartilaginous.

Braincase. Most parts of the braincase are known, and no fusion between individual elements is evident (Fig. 1 *C* and *D* and *SI Appendix*, Figs. S38 and S48). The anterior end of the cultriform process of the parasphenoid is unknown but the posterior end lacked teeth and was at least as wide as the foramen magnum (Fig. 1 *C* and *D*). A pair of internal carotid foramina is present, as in *Karaurus* and *Kokartus*, but they are located relatively close to the midline and face anteriorly, unlike *Karaurus* and *Kokartus* (19, 29). Internally there are two pairs of furrows that converge on a short, curved carotid canal: in one pair, the furrows are parasagittally oriented and directed caudally whereas in the other pair the furrows are orthogonal to the midline and are directed laterally (*SI Appendix*, Fig. S47). The orbitosphenoid (NMS G.2021.4.3) is rectangular in lateral view. The foramen for cranial nerve (CN) II is fully enclosed in bone as in cryptobranchids and many salamandroid salamanders (e.g., *Siren*, *Amphiuma*, *Plethodon*, and *Dicamptodon*) but unlike most hynobiids. The orientation of the foramen is also oblique as in cryptobranchids and *Siren*. There is also a notch for CN III (Fig. 1 *E* and *F*) as in *Pangerpeton* and some salamandroids (e.g., *Salamandra*, *Plethodon*, and *Dicamptodon*). The lateral edge of the orbitosphenoid was probably not exposed in dorsal view, unlike that in Cryptobranchoidea, and the ventromedial ends did not meet to form a sphenethmoid, thereby differing from the condition in most anurans. The prootic is similar in general structure to that of *Cryptobranchus* but the facet for the skull roof is directed dorsolaterally rather than dorsal and the facet for the pterygoid is directed ventrolaterally rather than lateral. The exoccipitals are unfused to the adjacent braincase elements (Fig. 1 *E* and *F*, *SI Appendix*, Figs. S38) as in most dissorophoids, and in proteid and some species of sirenid salamanders. The exoccipitals and opisthotic meet above and below a notch for CN X and the jugular vein (Fig. 1 *E* and *F*). However, the exoccipitals do not appear to meet one another either above or below the foramen magnum (*SI Appendix*, Fig. S38), as in the dissorophoid *Micropholis* (49), anurans, Cryptobranchidae, and Proteidae, but in contrast to the condition in *Doleserpeton* (50) and Gymnophiona (51). Elements potentially representing an operculum and stapes are known (*SI Appendix*, Figs. S48). The candidate stapes was associated with other braincase material but the operculum was not.

Lower jaw. The lower jaw of NMS G.2021.4.2 is articulated and almost complete (Fig. 1 *F*–*H* and *SI Appendix*, Fig. S4). The dentary is relatively long and extends posteriorly to a point close to the craniomandibular articulation (Fig. 1 *G* and *H*). The anterior end of the dentary forms a large oval symphyseal surface, as in other stem salamanders (Fig. 1 *G* and *H* and *SI Appendix*, Figs. S50–S51), including *Marmorerpeton* spp (33), and as also seen in cryptobranchids. The angular and prearticular are separate as in members of Cryptobranchoidea (*SI Appendix*, Figs. S52 and S53), but not in Salamandroidea (23). An elongate, toothed anterior coronoid element (*SI Appendix*, Fig. S54) sits inside the dentary tooth row (Fig. 1 *G* and *H*). A break part-way along this bone may be a suture (delimiting two separate elements) or possibly a physical break (indicating one single, broken element). The location and shape of this element (or pair of elements) resembles the coronoid reported for the fossil salamander *Qinglongtriton* (24), that of the extant Sirenidae and *Dicamptodon* (47), and the toothed element in the neotenic extant salamander *Ambystoma mexicanum* (*SI Appendix*, Fig. S79). A rhomboid, toothed element is preserved in the matrix dorsomedial to the prearticular and might represent the anterior part of the right pterygoid, a palatine, or a posterior coronoid similar to that of *Proteus* (*SI Appendix*, Figs. S55 and S79–S81).

Axial skeleton. The atlas of NMS G.2021.4.3 is complete and provides many characters for comparison with fossil salamanders known from isolated vertebrae (Fig. 2 *A*–*D*). As in some other stem-salamanders, the atlas has ovoid anterior cotyles, a small neural canal, a porous bone texture (*SI Appendix*, Figs. S57 and S58), a small odontoid process, no spinal nerve foramina, a neural crest, and a short neural arch that leaves a distinct gap between the base of the arch and the cotyles (25, 26). It resembles the atlas of *Kulgiherpeton* in all of the features listed above (25), but in *M. wakei*, the anterior end of the neural crest is broader (cf. *Ambystoma*) and the posterior zygapophyses are horizontal rather than oblique. The atlas of *M. wakei* is

Downloaded from https://www.pnas.org by UCL Library Services on July 25, 2022 from IP address 128.41.35.168.

proportionally longer than that of "Salamander A" (34) and *Egoria* (26). The odontoid process is more prominent than in *Urupia* (35). There is no indication of long transverse processes unlike *Regalerpeton* (52), small tubercle on the centrum unlike *Egoria*, *Kokartus*, *Kulgeriherpeton*, and *Qinglongtriton* (24–26), or flange on the neural arch unlike *Siren* and *Necturus* (53). The depression on the ventral surface of the centrum is shallow as in *Kulgeriherpeton* (25), rather than deep as in *Marmorerpeton kermacki* (33), or absent as in *Egoria* (26).

The dorsal vertebrae of *M. wakei* have a single neural spine with an unfinished apex (*SI Appendix*, Figs. S59–S62) that may extend beyond the level of the posterior end of the centrum. The base of the transverse processes involves both the centrum and neural arch, as also found in *Kokartus* (30) and most crown-salamanders but not salientians. The ventral surface can exhibit a midline depression (*SI Appendix*, Figs. S60–S62) as previously recorded for both *Marmorerpeton* and *Kokartus* (30, 33). The transverse processes of dorsal vertebrae, the sacrum, and first caudal are bifurcated, forming two distinct facets (*SI Appendix*, Figs. S59–S61) for bicapitate ribs (Fig. 2 *M* and *N*). The sacral rib is curved (*SI Appendix*, Figs. S62–S64). Nonbifurcated transverse processes are present on the first five caudal vertebrae (Fig. 2 *K*, *L*, and *O*). The first four caudal vertebrae represent caudosacrals as defined in (27) and as also reported for *Chunerpeton* and *Qinglongtriton* (27, 28). Most caudal vertebrae have long posteriorly projecting neural spines and even longer haemal arches (Fig. 2*O* and *SI Appendix*, Fig. S62 and S65–S67) that suggest a powerful tail for swimming.

Appendicular skeleton. The scapulocoracoid is tall and cylindrical, and the glenoid is buttress-like (Fig. 2 *E* and F and *SI Appendix*, Fig. S68). As in *Eocaecilia* (51), the coracoid foramen sits at the ventral edge of the bone and the foramen would have been completed in cartilage, as shown by the unfinished ventral margins. The only available humerus is badly crushed but has a distinct deltopectoral crest (*SI Appendix*, Fig. S69). The ilium has an acetabulum that is stepped and a shaft that is mainly vertical and flared at its end (Fig. 2*G* and *SI Appendix*, Fig. S70). The ischia are paired with a curved lateral edge similar to that in many extant salamanders (Fig. 2 *H* and *I*). The femur is expanded at both ends, bears a ventral trochanter and a small posteroventral crest (Fig. 2*J* and *SI Appendix*, Fig. S71) similar to that of crown salamanders such as *Cryptobranchus* and *Andrias* (54) but the crest is shorter. The fibula has a bilobate proximal end and a longitudinal ridge, and the tibia is proximally wide (*SI Appendix*, Fig. S72): both bones resemble those of *Doleserpeton* (46). Metapodials and curved terminal phalanges are also preserved (*SI Appendix*, Figs. S73 and S74) but no carpals or tarsal elements have been recovered and these elements were presumably unossified.

Phylogenetic Analysis. We constructed a morphological dataset to test the hypothesized affinities of early fossil salamanders. Our taxon sample has unprecedented representation for studies of salamander evolution (*SI Appendix*, Table S10), spanning the likely stem-lissamphibians and a broad range of the salamander total-group: 7 dissorophoids, 9 nonurodele lissamphibians, 17 fossil salamanders and 22 extant salamanders (representing all 10 living families) (*SI Appendix*, Part F). Of these, we conducted high-resolution CT scans of 15 extant salamander species, allowing comprehensive study and recoding of comparative skeletal anatomy relevant to higher-level relationships (data available at https://www.morphosource.org/projects/00000C868). Our character list combines data from analyses of broader lissamphibian relationships (20), fossil salamanders (23), and living salamanders (53), providing an inclusive test of the affinities of Mesozoic fossil salamanders to the stem-lineage or crown-group (*SI Appendix*, Part G). Complex, multistate characters from previous studies were subdivided into independently varying character statements to better analyze the relationship among states. Our analyses used a well-established molecular topology (55) as a backbone constraint for the relationships among all extant taxa except *Ranodon* (*SI Appendix*, Part H).

Bayesian analysis under a relaxed MkV model of character state transitions, using fossil ages (*SI Appendix*, Part I) in the context of a fossilized-birth-death (FBD) model (*SI Appendix*, Part J), returns a phylogenetic hypothesis, with greater membership of the salamander stem-lineage than has previously been suggested, and includes *Marmorerpeton* as the sister taxon to *Kokarkus* within the clade Karauridae (Fig. 3). The Triassic genus *Triassurus* was the sister taxon to all other members of Caudata. Crownward of *Triassurus*, we find a major division between a clade that includes *Pangerpeton* + crown-group salamanders, and a previously unrecognized clade of stem-salamanders that includes Karauridae (*Marmorerpeton* + *Kokarkus* + *Karaurus*) plus several fossil taxa from the Jurassic-Cretaceous of Eurasia. *Iridotriton*, *Linglongtriton*, *Neimongotriton*, and *Regelerpeton* are in a polytomy with Cryptobranchoidea and the clade comprising all other crown-group salamanders (Salamandroidea + Sirenidae; Fig. 3). They may therefore be either crownward stem-salamanders or early members of the crown-group.

Our results differ from those of previous analyses, which recovered most Mesozoic taxa (except for karaurids) as crown salamanders, either as stem-salamandroids [*Beiyanerpeton* and *Qinglongtriton* (21, 23, 24, 27, 28)] or stem-cryptobranchoids [*Chunerpeton* (21, 23, 24, 27)]. The finding of a close relationship among *Chunerpeton*, *Beiyanerpeton*, and *Qinglongtriton* is consistent with the observation that they have relatively similar anatomy (28). Synapomorphies of the new Mesozoic Eurasian clade include monocuspid tooth crowns, a squamosal with a ventral process that is oriented anteroventrally, and a parasphenoid that widens anteriorly (Fig. 4). *Beiyanerpeton*, *Qinglongtriton*, and Karauridae also share bicapitate ribs and an interparietal seam that is irregular. Posterior support levels for this Mesozoic Eurasian clade are strong but not exceptional (0.88). Therefore, discovery of further fossil material may modify inferred relationships, potentially by demonstrating that the inferred synapomorphies of the new clade (e.g., monocuspid tooth crowns, cultriform process anteriorly wide, and dentary labial groove) are, in fact, plesiomorphies or homoplasies that instead characterize a paraphyletic (neotenic) grade outside the crown-group. Nevertheless, this clade is still recovered by an analysis excluding 36 characters associated with neoteny, albeit with reduced support (0.58; *SI Appendix*, Fig. S85). It is also still recovered if *Triassurus* is removed from the analysis (0.80; *SI Appendix*, Fig. S86).

More detailed descriptions of the fossil taxa from China (including high resolution and well-lit images of the vertebral anatomy) may help resolve this issue.

Marmorerpeton is included in Karauridae with high posterior probability (1.0) and shares several synapomorphies with other members of the clade (*Kokartus*, *Karaurus*), including an interorbital distance greater than the width of the orbit, a posterolateral process of the prefrontal, heavy sculpture on the skull roofing bones, and vertebral cotyles that are greater in diameter than the neural canal.

The phylogenetic topology within Caudata is unaffected by inclusion or exclusion of the enigmatic Albanerpetontidae (*SI Appendix*, Figs. S83 and S84), an extinct clade of possible lissamphibians (56). When included, albanerpetontids are found

Downloaded from https://www.pnas.org by UCL Library Services on July 25, 2022 from IP address 128.41.35.168.

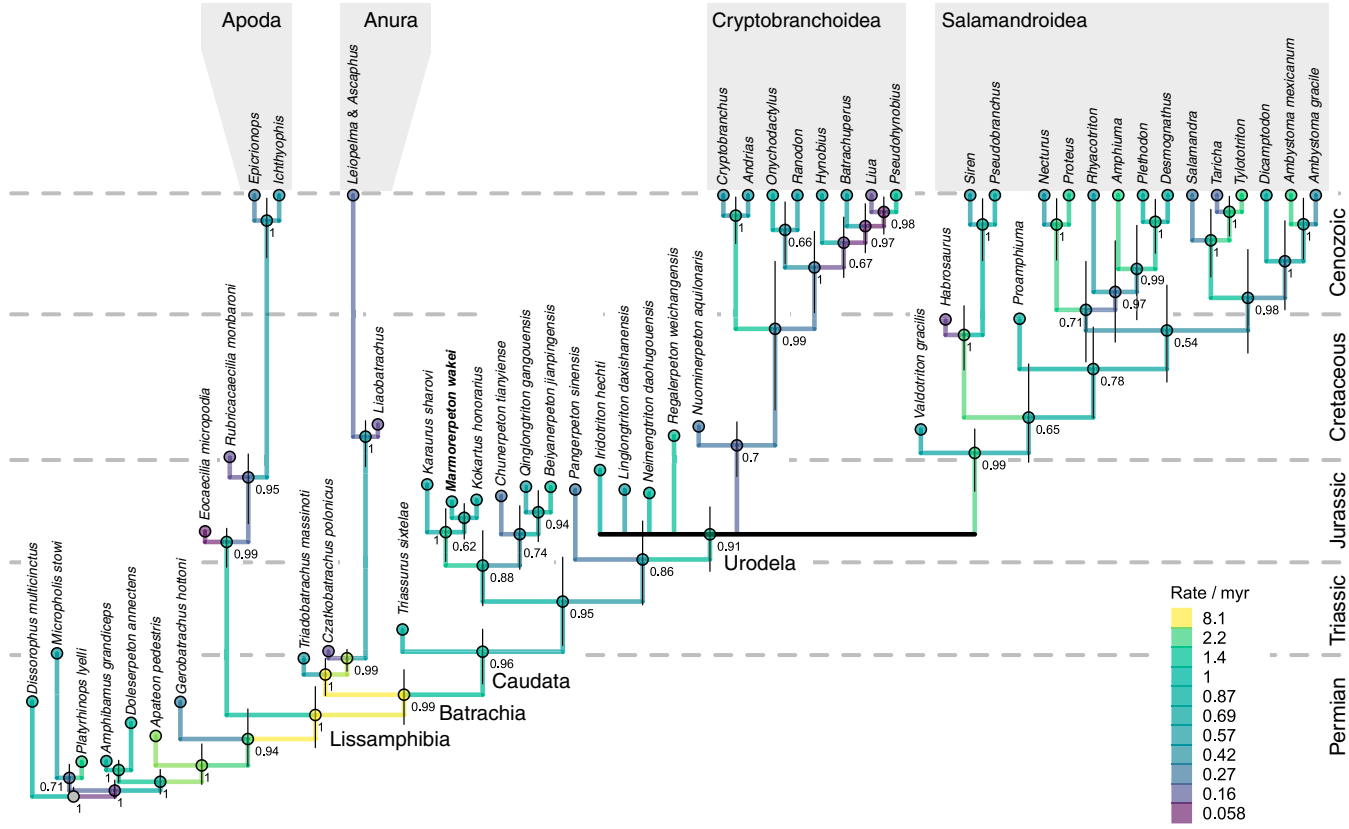

Fig. 3. Phylogenetic relationships of *Marmorerpeton* based on analysis of 53 taxa (Albanerpetontidae and *Liaoxitriton zhongjiani* excluded) using 308 characters (*SI Appendix*, Part F and G), with a constraint tree for 24 of the 25 extant taxa (*SI Appendix*, Part H) in a Bayesian framework under a relaxed MkV model of character state transitions, using fossil ages (*SI Appendix*, Part I) in the context of a fossilized-birth-death (FBD) model (*SI Appendix*, Part J). Branch lengths are scaled to units of time. Posterior probabilities are shown adjacent to nodes. *Marmorerpeton* (shown in bold) is placed as the sister taxon to *Kokartus* within Karauridae. Colors show the rate of change for the characters included in the analysis. Several fossil taxa previously referred to Hynobiidae are placed outside Cryptobranchoidea in a polytomy with Urodela. *Chunerpeton*, which has previously been used to constrain crown-group Cryptobranchoidea (76–78), is placed on the stem. Note that Salamadroidea includes Sirenidae as in (21).

to be the sister-group of Caudata. However, we note great uncertainty regarding albanerpetontid affinities and that this issue requires further investigation.

***Neoteny and aquatic habits in* Marmorerpeton.** Our observations support previous suggestions of cryptobranchid-like neoteny in *Marmorerpeton* and some other stem salamanders (29, 33, 57). Among extant salamanders, several species are regarded as neotenic because they reproduce while retaining their aquatic larval form (47, 53). This is a life history strategy which may be obligate (e.g., Sirenidae, Proteidae) or facultative in response to the environment (e.g., *Triturus*, *Dicamptodon*) (58). However, the extent to which particular taxa exhibit or retain pedomorphic traits (such as external gills) as adults is variable (47, 53) [e.g., adult cryptobranchids show many pedomorphic traits but their skulls are well developed and their external gills are reduced through ontogeny (3, 53)].

Marmorerpeton exhibits several traits previously inferred to be pedomorphic based on their presence in both larvae of transforming species and in adults of nontransforming species (33, 47, 53): a vomerine tooth row at the labial edge of the bone, a toothed anterior coronoid bone, an anterodorsal fenestra (between the premaxilla and nasal), and a pterygoid tooth row, as well as possibly the absence of the lacrimal and palatine, the presence of weakly pedicellate teeth (33), and a reduced maxilla. These traits are also found among other members of the Eurasian stem salamander clade: *SI Appendix*, Part L). One of the smaller specimens of *M. wakei* (NMS G.2021.4.2) includes a short string of tooth-like structures that may be branchial denticles (indicating the presence of external gills or gill slits) (*SI Appendix*, Fig. S56), as found in other neotenic fossil salamanders *Chunerpeton* (28), *Beiyanerpeton* (22), *Qinglongtriton* (24), and *Triassurus* (20), premetamorphic or neotenic dissorophoids (42, 44, 59), and juvenile cryptobranchids. However, various traits found in pedomorphic salamandroids (e.g., loss of the maxilla, nasal, and prefrontals, a rectangular pterygoid) are not evident in *Marmorerpeton*. Therefore, the combination of characters present in *Marmorerpeton* and other members of the Eurasian clade suggest that these taxa had a form of neoteny and lifestyle similar to that found in extant members of Cryptobranchidae (53).

The long tail with tall, posteriorly directed neural spines, regular sculpture (60), enlarged first metatarsal/metacarpal (61), likely absence of ossified carpals and tarsals, and limb bones with unfinished ends (62) are consistent with aquatic life but, as in Cryptobranchidae, the limb elements do show some ridges and processes related to muscle attachment (54). The relatively broad skull shape, the dorsoventrally shallow skull profile, anterolateral location of the orbits, and robust jaws also resemble features of cryptobranchids: a clade that includes the largest living amphibians (3, 63). These animals live in streams as sit-and-wait ambush predators, using suction feeding, with expansion of the oropharyngeal volume, to capture prey (3), and forceful bites to immobilize it (3, 63). This type of feeding appears to have evolved repeatedly and is also inferred for

Downloaded from https://www.pnas.org by UCL Library Services on July 25, 2022 from IP address 128.41.35.168.

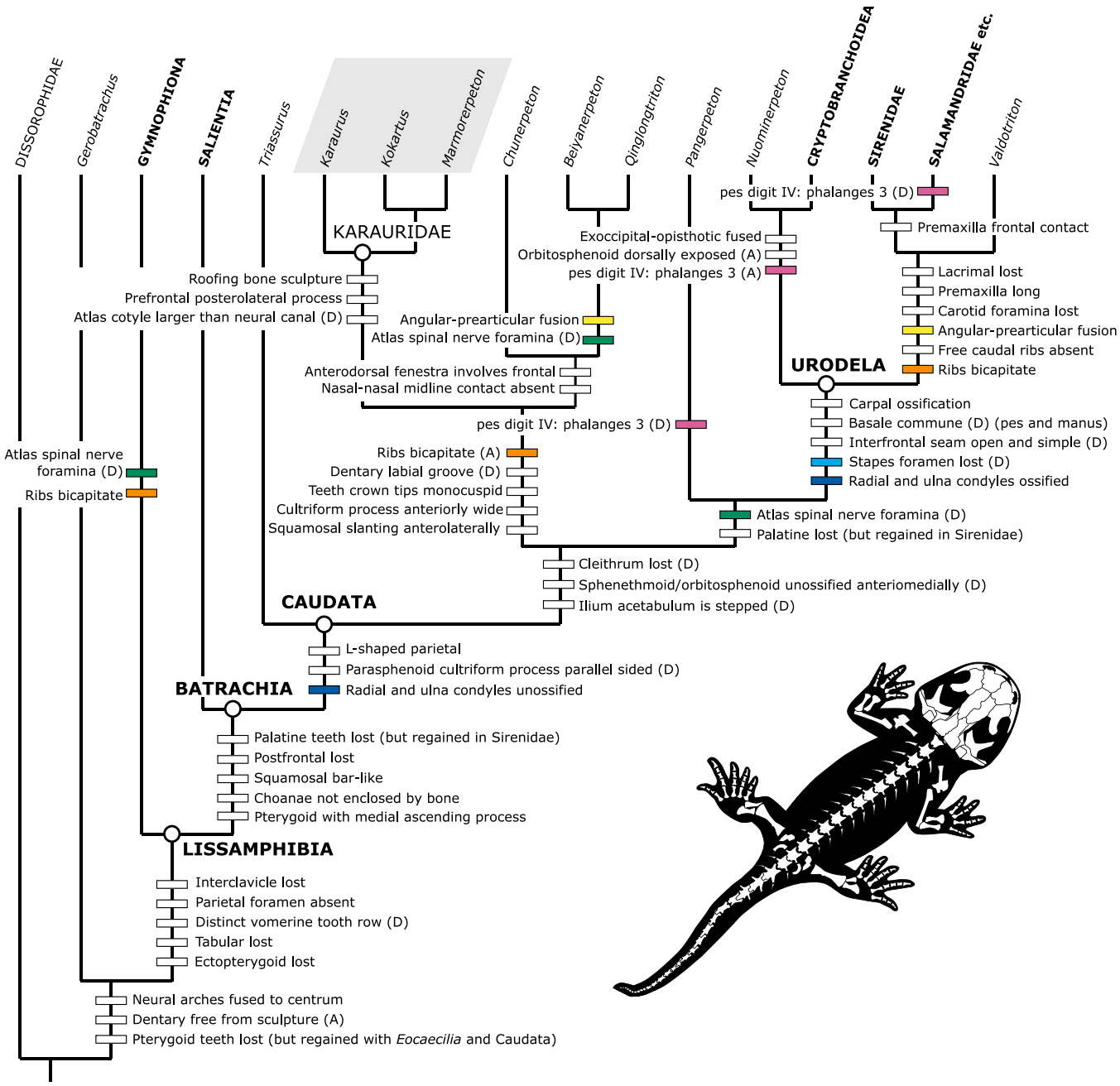

Fig. 4. Character evolution in Lissamphibia with a focus on early salamanders and characters discussed in the text. Major groups in capital letters. Extant taxa in bold. Karauridae is indicated by a gray box. Apomorphies inferred by our main analysis are indicated by rectangles on branches just outside the relevant node. Some of these are rectangles are colored to indicate the same character (which in some cases shows a reversal or convergent evolution). *Marmorerpeton* is nested within Karauridae outside crown salamanders (Urodela). A, ACCTRAN; D, DELTRAN.

Permian and Mesozoic temnospondyls (3, 63). Unlike those of cryptobranchoids and most crown salamanders, the jaw muscles of *Marmorerpeton* and other members of Karauridae (29) did not extend onto the dorsal surface of the skull table—a plesiomorphy that is also shared with other temnospondyls.

Discussion

Stem Salamander Neoteny and Diversity. We find eight fossil salamanders on the stem of Caudata. Seven of these are neotenic, aquatic forms and include a range of body and skull shapes suggestive of ecological diversity: large-bodied species with wide heads [e.g., *Beiyanerpeton*, skull = 30 × 42 mm (21); *Karaurus*, skull = ~40 × 50 mm (19)]; large-bodied species with narrower heads [e.g., *Marmorerpeton*, skull = 32 × 33; *Qinglongtriton*, skull = 39 × 38 mm (24)]; and *species*, known only from larval individuals with a wide head [e.g., *Triassurus*, skull length = ~5.5 mm, skull width = ~7.5 mm (20)]. The remaining stem-taxon and sister to the crown is short-bodied and metamorphosed (i.e., not neotenic) with a wide head [e.g., *Pangerpeton*, skull = 8 × 13 mm (64)] (*SI Appendix*, Part J).

Late Jurassic-Early Cretaceous crown-group salamanders include both neotenic and nonneotenic taxa. Nonneotenic taxa include *Nuominerpeton*, *Valdotriton*, and the possible crown-group member *Linglongtriton*, which have small bodies with skull lengths and widths less than 25 mm (23, 65, 66). Neotenic taxa include *Hylaeobatrachus croyi* (Barremian/Albian, Belgium) and a possibly related taxon from Spain (Barremian, Las

Downloaded from https://www.pnas.org by UCL Library Services on July 25, 2022 from IP address 128.41.35.168.

Hoyas) (65). These findings suggest that neoteny, which was important in dissorophoids (42, 67), was also important to the earliest salamanders, as it is to many crown members today (14, 58, 68).

The Evolution of Salamanders. Compared to many previous studies, our data provide a relatively complete test of the relationships of *Karaurus*, and many other fossil salamanders relative to the major crown-group lineages, Cryptobranchoidea and Salamandroidea [including Sirenidae as in (21)]. We achieved this outcome by extensively sampling taxa that span from the Permian to the present (*SI Appendix*, Part F) and by including relevant characters from multiple analyses with different taxonomic foci (20, 23, 53) (*SI Appendix*, Part G). *Karaurus*, from the Late Jurassic of Kazakhstan has frequently been used as the single outgroup in studies of salamander phylogeny, thereby having a strong effect on inferred polarities of character states for the salamander crown-group (*SI Appendix*, Part M) (21, 23, 24, 27, 28). This restricted sampling is potentially problematic because *Karaurus* has also been found as a crown-group salamander within, or as the sister taxon to, Cryptobranchoidea (69), and is morphologically specialized, as described above. Moreover, some studies with broad sampling of Lissamphibia report uncertainties regarding the placement of *Karaurus* [as "highly ambiguous" (53)].

Our analysis recovered several taxa (e.g., *Beiyanerpeton*, *Qinglongtriton*, and *Chunerpeton*) (Fig. 3) previously hypothesized to be members of the crown-group, as instead belonging in the stem-group. This placement of *Beiyanerpeton* and *Qinglongtriton* contradicts previous analyses (21, 23, 24, 27, 28) that recovered these taxa on the stem of Salamandroidea, but may resolve previous doubts expressed regarding their affinities (28).

Our results have implications for calibrations of the minimum ages of the cryptobranchoid and salamandroid crown-groups (Fig. 3). Our finding of *Chunerpeton* as a stem-salamander strengthens doubts regarding its cryptobranchid affinity (28, 70, 71) and argues against its widespread use as a molecular constraint to calibrate the cryptobranchoid crown-group node (9, 14, 71–81) (SI Appendix, Part N). Our analysis also places *Iridotrition*, *Linglongtriton*, *Neimengtriton*, and *Regalerpeton* (previously referred to the stem of Hynobiidae, and therefore within the cryptobranchoid crown-group) (23, 24, 27, 52, 66) in an unresolved polytomy with Cryptobranchoidea and Salamandroidea. *Nuominerpeton* is placed outside Cryptobranchidae + Hynobiidae, as a stem cryptobranchoid. This result implies that the oldest confident record of the cryptobranchoid crown group so far may be isolated elements reported from the Upper Paleocene of North America and Mongolia such as *Cryptobranchus saskatchewanesis* (82) or *Aviturus exsecratus* (83). A younger divergence time for Cryptobranchoidea fits better with some molecular estimates (68, 69, 71, 84). Resolution of this issue requires greater anatomical and comparative analysis of the available Cretaceous and Cenozoic fossil specimens.

Our phylogenetic hypothesis suggests that the salamander crown-group may have originated by the Late Jurassic (Fig. 3). The oldest candidate crown-group salamanders are *Linglongtriton* and *Neimengtriton* from the early Late Jurassic of China, which are placed with uncertainty either just inside or just outside Urodela [161.2–150.8 Ma for *Linglongtriton* (23)]. This age is only slightly younger than the age range estimated (220–160 Ma) for the origin of crown-salamanders, as inferred by an analysis restricted to calibrations outside Lissamphibia (84). Whether older isolated bones from the Middle Jurassic of Siberia, named *Kiyatriton krasnolutskii* (36), represent a stem- or crown-group salamander deserves further study.

We find *Habrosaurus* [Late Cretaceous to Paleocene, 84.9–58.7 Ma, USA (85)] and *Proamphiuma* [Late Cretaceous to Paleocene, 70.6–63.3 Ma, USA (86)] within the salamandroid crown group (Fig. 3), as is widely accepted. However, we find *Valdotriton*, from the Lower Cretaceous, 130.0–125.45 Ma, of Spain (65), previously placed as a crown-salamandroid (21, 23, 24), on the stem-lineage of Salamandroidea (Fig. 3), cautioning against using it as a calibration for the salamandroid crown group (67, 80) (*SI Appendix*, Part N).

The fossils and analyses described here strengthen the possibility that several key characters might have a more complex evolution than previously recognized (Fig. 4). First, the presence of atlantal spinal nerve foramina has long been considered a diagnostic feature of crown-group salamanders due to its presence in all extant salamanders but absence in anurans, *Marmorerpeton*, *Karaurus*, and *Kokartus* (33). However, this foramen is present in the atlas of *Beiyanerpeton* and *Qinglongtriton* and also in the stem-caecilians *Rubricacaecilia* and *Eocaecilia* (51, 87). Thus, the foramen may have been gained or lost independently within Caudata. Second, unicapitate ribs have been considered diagnostic for Cryptobranchoidea (23), and this character state was considered important in previous phylogenetic interpretations of *Chunerpeton* (27). However, this trait is also present in salientians, *Triassurus*, and albanerpetontids (17, 20, 56), suggesting that it may actually represent a plesiomorphic character state for Caudata. Correspondingly, bicapitate ribs appear to be a synapomorphy for the Eurasian stem salamander clade as well as Salamandroidea + *Valdotrition* and, potentially, Gymnophiona. Third, the fusion of the angular and prearticular which occurs in Salamandroidea (23) may also have arisen independently in *Beiyanerpeton* and *Qinglongtriton*. Fourth, unossified radial and ulnar condyles appear to represent synapomorphies for total-group salamanders (Caudata) whereas ossified radial and ulnar condyles appear to represent a synapomorphy for crown-group salamanders (Urodela). Fifth, a reduction to four phalanges on digit IV of the pes (although variable in *Chunerpeton* and *Onychodactylus*) (88) may represent an apomorphy for both Cryptobranchoidea and clades within Salamandroidea (Fig. 3). Sixth, the presence of small supratemporal bones in *Marmorerpteon* is perhaps consistent with suggestions that these bones are present in the frog *Pelobates* but are incorporated into the medial part of the squamosal in most batrachians (89, 90). Whether these bones have been plesiomorphically retained in *Marmorerpteon* or have reappeared due to accelerated somatic development will require additional sampling of the fossil record.

The *Marmorerpeton wakei* material described here also described here contributes to the number and range of characters that we can compare among fossil taxa. It includes well-preserved 3D examples of key skeletal elements including the atlas, scapulocoracoid, ilium, and orbitosphenoid (represented by 43 characters in our dataset). The unique combination of characters states exhibited by these elements emphasizes the importance of fossils and raises the possibility that no living salamander retains the plesiomorphic condition of the girdle or braincase, highlighting the potential of fossils for understanding morphological evolution and character polarity.

Our results help clarify our understanding of stepwise lissamphibian character assembly (Fig. 4). Compared to dissorophoids, Lissamphibia have a long and distinct vomerine tooth row (less than six teeth) but have lost the ectopterygoid, tabulars, interclavicle, and parietal foramen (Fig. 4). Our results are also consistent with suggestions that early Lissamphibia were characterized by gracile, elongate ilia (20); although an ilium was not referred to *Eocaecilia*, a long blade like-element was

Downloaded from https://www.pnas.org by UCL Library Services on July 25, 2022 from IP address 128.41.35.168.

associated with the material (51). Batrachian apomorphies include a bar-like ventral process of the squamosal, choanae not enclosed by bone, and loss of both palatine teeth and the postfrontal (Fig. 4). Our results support recent suggestions that caudate apomorphies include an L-shaped parietal and a parasphenoid with a broad parallel-sided cultriform process (20). We also find that Caudata may be characterized by an ilium with a stepped acetabulum and radial and ulna condyles that are unossified. Apomorphies for crown-group salamanders (Urodela) may include a simple interfrontal suture seam and ossification of at least some carpal/tarsal bones. Several apomorphies are also indicated for Salamandroidea including the absence of caudal ribs and a premaxilla with an elongate alary process that contacts the frontal.

Conclusions. The history of investigating major evolutionary transitions includes many examples of analyses that have relied heavily on single taxa (e.g., early tetrapods, *Ichthyostega*; salientians, *Triadobatrachus massinoti*; birds, *Archaeopteryx lithographica*; and hominoids, *Australopithecus afarensis*). Such taxa are often the most complete fossils known and provide valuable examples of ancient character combinations not found in any extant taxon. However, analyses of additional taxa have invariably contributed to our understanding and often overturn long-held hypotheses (18, 91–93). Just as analyses of bird origins have become less reliant on *Archaeopteryx* (94), we anticipate that future analyses of salamanders will become less reliant on *Karaurus*. All taxa are a complex mixture of plesiomorphic and derived characters reflecting adaptation to a particular niche, making it unlikely that any one taxon is a perfect intermediate form.

The new specimens of *Marmorerpeton* add considerably to knowledge of stem-salamander anatomy and diversity. Exceptional anatomical resolution and detail from our 3D scans help resolve character state polarities and the sequence of acquisition of anatomical traits on the salamander stem lineage. These data are crucial to understanding deep divergences in the salamander crown-group, as well as the affinities of other fossil species to either the crown- or stem-lineage. Our analyses provide evidence for a Eurasian radiation of relatively large aquatic neotenic stem-salamanders. Within this radiation, *Marmorerpeton* and other karaurids represent a relatively robustly-built group with conspicuous skull-roof sculpture, spanning the Middle–Late Jurassic, and possibly Early Cretaceous (25). However, many questions as to the origins and relationships of early lissamphibians remain unanswered because we lack detailed information on other taxa, including stem frogs, Triassic salamanders, albanerpetontids, and caecilians, as well as outgroups such as *Gerobatrachus*. Future studies reporting this type of data will be central to resolving long-standing uncertainties about the early evolution of Batrachia and Lissamphibia.

Materials and Methods

The new specimens are accessioned at National Museums Scotland, Edinburgh, UK (NMS) and were micro-CT-scanned at the University of Bristol using a Nikon XT H 225 ST with a peak energy of 222 kV and peak current of 375. Scan parameters are given in *SI Appendix*, Table S6, and also accompany the scan data and 3D models at MorphoSource (37). Most models were generated from volumes with a voxel size of 0.020 mm or less (*SI Appendix*, Table S5). Specimens were segmented using Amira 6.7.0, and a restoration of the skull was assembled and imaged using Blender 2.92. Fifteen specimens representing 15 species of extant salamanders were also segmented as part of the comparative sample (*SI Appendix*, Part F) and the scan data and models are available at MorphoSource (95).

Our phylogenetic analysis involved 55 OTUs and 308 characters (*SI Appendix*, Part G). The OTUs included 7 dissorophoids, 9 nonurodele lissamphibians, 17 fossil salamanders, and 22 extant salamanders (*SI Appendix*, Part F). *Liaoxitriton zhongjiani* was removed from our final analyses due to its highly unstable phylogenetic position (*SI Appendix*, Fig. S85). We also ran analyses including and excluding Albanerpetontidae, which did not influence in-group results (*SI Appendix*, Figs. S84 and S85). Most characters were adapted from three previous major studies (20, 23, 53). Phylogenetic analyses were conducted in MrBayes 3.2 (96) under a relaxed MkV model of character state transitions with independent gamma branch rates and a fossilized-birth-death tree prior (97) [analytical script available on the Open Science Framework (OSF) (98)]. The tree age prior was set to a uniform distribution between 312 and 330 Ma, based on the ages of *Micropholis stowi* and *Platyrhinops lyelli*. Taxon ages were drawn from uniform distributions between their oldest and youngest possible occurrence ages, reflecting stratigraphic uncertainty (*SI Appendix*, Part I), and relationships among extant salamanders, frogs and caecilians were constrained using a backbone tree from (55) (*SI Appendix*, Part H). Analyses were run for 15 million generations, discarding the first 25% as burn-in, and convergence metrics suggest that runs generally converged before six million generations. The full script including the data matrix and parameter priors is available in (*SI Appendix*, Part J). Character optimization was executed in PAUP* 4.0a169 (99)

Data Availability. Original data created for the study have been deposited in a persistent repository (Morphosource) and will be available upon publication (37, 95). The analytical script is available on the OSF (98).

ACKNOWLEDGMENTS. This study received funding from Leverhulme Research Project Grant RPG-2018-381 (Project 550474; award no. 178055). We thank John Muir Trust for access to the Elgol Coast Site of Special Scientific Interest, and NatureSco for granting permits. The study of Russian specimens is funded by the Russian Foundation for Basic Research (Project 19-04-00060 to P.S.). Funding from an endowment to Oxford University from the Vladimir Potanin Foundation was used to employ a student to conduct segmentation of some fossil material and to facilitate collaboration between P.S. and the UK researchers. For assistance with CT scanning, we thank Tom Davies (University of Bristol). For help with fieldwork and specimen discovery, we thank Roger Close, Richard Butler, Andrzej Wolniewicz, and, in particular, Daniel Field who found NMS G.2021.4.2. For access to comparative materials, we thank Mathew Lowe, Jason Head, Jeff Streicher, Eileen Westwig, Mark Carnall, and Mike Day. For correspondence and discussion regarding Lissamphibia, we thank Ana Serra Silva, Mark Wilkinson, Hendrik Müller, Stephen Mahony, Eduardo Ascarrunz, Veniamin Kolchanov, Natalie Cooper, and Rainer Schoch. For help with *SI Appendix*, Figs. S1–S5, we thank Lizzy Griffiths. For YouTube Blender tutorials, we thank Grant Abbit, Josh Gambrell, CGRogue, and Blender Guru. For discussion regarding Latin names, we thank Mairéad McAuley. We also thank two reviewers for their feedback and suggestions which greatly improved this study.

Author affiliations: [a]Cell and Developmental Biology, University College London, London, WC1E 6BT, United Kingdom; [b]Department of Earth Sciences, University of Oxford, Oxford, OX1 3AN, United Kingdom; [c]Vertebrate Zoology Department, Saint Petersburg State University, Saint Petersburg,199034, Russia; [d]Greenshaw High School, Sutton, SM1 3DY, United Kingdom; [e]Oxford University Museum of Natural History, Oxford University, Oxford, OX1 3PW, United Kingdom; and [f]Department of Natural Sciences, National Museums Scotland, Edinburgh, EH1 1JF, United Kingdom

1. R. D. Davic, H. H. Welsh, On the ecological roles of salamanders. *Annu. Rev. Ecol. Evol. Syst.* **35**, 405–434 (2004).
2. P. D. Moldowan *et al.*, Nature's pitfall trap: Salamanders as rich prey for carnivorous plants in a nutrient-poor northern bog ecosystem. *Ecology* **100**, e02770 (2019).
3. E. Heiss, N. Natchev, M. Gumpenberger, A. Weissenbacher, S. Van Wassenbergh, Biomechanics and hydrodynamics of prey capture in the Chinese giant salamander reveal a high-performance jaw-powered suction feeding mechanism. *J. R. Soc. Interface* **10**, 20121028 (2013).
4. N. M. Ledbetter, R. M. Bonett, Terrestriality constrains salamander limb diversification: Implications for the evolution of pentadactyly. *J. Evol. Biol.* **32**, 642–652 (2019).
5. S. Reinhard, S. Voitel, A. Kupfer, External fertilisation and paternal care in the paedomorphic salamander *Siren intermedia* Barnes, 1826 (Urodela: Sirenidae). *Zool. Anz.* **253**, 1–5 (2013).
6. D. B. Wake, What salamanders have taught us about evolution. *Annu. Rev. Ecol. Evol. Syst.* **40**, 333–352 (2009).

Downloaded from https://www.pnas.org by UCL Library Services on July 25, 2022 from IP address 128.41.35.168.

7. C. A. Boisvert, Vertebral development of modern salamanders provides insights into a unique event of their evolutionary history. *J. Exp. Zoolog. B Mol. Dev. Evol.* **312**, 1–29 (2009).
8. N. B. Fröbisch, Ossification patterns in the tetrapod limb–conservation and divergence from morphogenetic events. *Biol. Rev. Camb. Philos. Soc.* **83**, 571–600 (2008).
9. R. M. Bonett, N. M. Ledbetter, A. J. Hess, M. A. Herrboldt, M. Denoël, Repeated ecological and life cycle transitions make salamanders an ideal model for evolution and development. *Dev. Dyn.* **251**, 957–972 (2022).
10. J. W. Godwin, A. R. Pinto, N. A. Rosenthal, Macrophages are required for adult salamander limb regeneration. *Proc. Natl. Acad. Sci. U.S.A.* **110**, 9415–9420 (2013).
11. A. Joven, A. Elewa, A. Simon, Model systems for regeneration: salamanders. *Development* **146**, dev167700 (2019).
12. S. M. Kawano, R. W. Blob, Propulsive forces of mudskipper fins and salamander limbs during terrestrial locomotion: implications for the invasion of land. *Integr. Comp. Biol.* **53**, 283–294 (2013).
13. A.-C. Fabre *et al.*, Metamorphosis shapes cranial diversity and rate of evolution in salamanders. *Nat. Ecol. Evol.* **4**, 1129–1140 (2020).
14. R. M. Bonett, A. L. Blair, Evidence for complex life cycle constraints on salamander body form diversification. *Proc. Natl. Acad. Sci. U.S.A.* **114**, 9936–9941 (2017).
15. S. Schloissnig *et al.*, The giant axolotl genome uncovers the evolution, scaling, and transcriptional control of complex gene loci. *Proc. Natl. Acad. Sci. U.S.A.* **118**, e2017176118 (2021).
16. T. Lüddecke, S. Schulz, S. Steinfartz, M. Vences, A salamander's toxic arsenal: Review of skin poison diversity and function in true salamanders, genus *Salamandra*. *Naturwissenschaften* **105**, 56 (2018).
17. E. Ascarrunz, J.-C. Rage, P. Legreneur, M. Laurin, *Triadobatrachus massinoti,* the earliest known lissamphibian (Vertebrata: Tetrapoda) re-examined by μCT scan, and the evolution of trunk length in batrachians. *Contrib. Zool.* **85**, 201–234 (2016).
18. S. E. Evans, M. Borsuk-Białynicka, The Early Triassic stem-frog *Czatkobatrachus* from Poland. *Palaeontol. Pol.* **65**, 79–105 (2009).
19. M. F. Ivakhnenko, Urodeles from the Triassic and Jurassic of Soviet Central Asia. *Paleontologičeskij žurnal* **1978**, 89 (1978).
20. R. R. Schoch, R. Werneburg, S. Voigt, A Triassic stem-salamander from Kyrgyzstan and the origin of salamanders. *Proc. Natl. Acad. Sci. U.S.A.* **117**, 11584–11588 (2020).
21. K.-Q. Gao, N. H. Shubin, Late Jurassic salamandroid from western Liaoning, China. *Proc. Natl. Acad. Sci. U.S.A.* **109**, 5767–5772 (2012).
22. K. Q. Gao, N. H. Shubin, Late Jurassic salamanders from northern China. *Nature* **410**, 574–577 (2001).
23. J. Jia, K.-Q. Gao, A new stem hynobiid salamander (Urodela, Cryptobranchoidea) from the Upper Jurassic (Oxfordian) of Liaoning Province, China. *J. Vertebr. Paleontol.* **39**, e1588285 (2019).
24. J. Jia, K.-Q. Gao, A new basal salamandroid (Amphibia, Urodela) from the Late Jurassic of Qinglong, Hebei Province, China. *PLoS One* **11**, e0153834 (2016).
25. P. P. Skutschas *et al.*, A new relict stem salamander from the Early Cretaceous of Yakutia, Siberian Russia. *Acta Palaeontol. Pol.* **63**, 519–525 (2018).
26. P. Skutschas *et al.*, A new small-sized stem salamander from the Middle Jurassic of Western Siberia, Russia. *PLoS One* **15**, e0228610 (2020).
27. J. Jia, J. S. Anderson, K.-Q. Gao, Middle Jurassic stem hynobiids from China shed light on the evolution of basal salamanders. *iScience* **24**, 102744 (2021).
28. Y.-F. Rong, D. Vasilyan, L.-P. Dong, Y. Wang, Revision of *Chunerpeton tianyiense* (Lissamphibia, Caudata): is it a cryptobranchid salamander? *Palaeoworld* **30**, 708–723 (2020).
29. P. Skutschas, T. Martin, Cranial anatomy of the stem salamander *Kokartus honorarius* (Amphibia: Caudata) from the Middle Jurassic of Kyrgyzstan. *Zool. J. Linn. Soc.* **161**, 816–838 (2011).
30. A. O. Averianov, T. Martin, P. P. Skutschas, A. S. Rezvyi, A. A. Bakirov, Amphibians from the Middle Jurassic Balabansai Svita in the Fergana Depression, Kyrgyzstan (central Asia). *Palaeontology* **51**, 471–485 (2008).
31. J. D. Pardo, B. J. Small, A. K. Huttenlocker, Stem caecilian from the Triassic of Colorado sheds light on the origins of Lissamphibia. *Proc. Natl. Acad. Sci. U.S.A.* **114**, E5389–E5395 (2017).
32. P. P. Skutschas, Y. M. Gubin, A new salamander from the Late Paleocene–Early Eocene of Ukraine. *Acta Palaeontol. Pol.* **57**, 135–148 (2012).
33. S. E. Evans, A. R. Milner, F. Mussett, The earliest known salamanders (Amphibia, Caudata): A record from the Middle Jurassic of England. *Geobios* **21**, 539–552 (1988).
34. E. Panciroli *et al.*, Diverse vertebrate assemblage of the Kilmaluag Formation (Bathonian, Middle Jurassic) of Skye, Scotland. *Earth Environ. Sci. Trans. R. Soc. Edinb.* **111**, 135–156 (2020).
35. P. P. Skutschas, S. A. Krasnolutskii, A new genus and species of basal salamanders from the Middle Jurassic of Western Siberia, Russia. *Proc. Zool. Inst. RAS* **315**, 167–175 (2011).
36. P. P. Skutschas, A new crown-group salamander from the Middle Jurassic of Western Siberia, Russia. *Palaeobiodivers. Palaeoenviron.* **96**, 41–48 (2016).
37. M. E. H. Jones *et al.*, Middle Jurassic fossils document an early stage in salamander evolution. MorphoSource. https://www.morphosource.org/projects/000397563. Deposited 8 March 2019.
38. S. E. Evans, M. Waldman, Small reptiles and amphibians from the Middle Jurassic of Skye, Scotland. *Mus. North. Ariz. Bull.* **60**, 219–226 (1996).
39. J. E. Andrews, The sedimentary facies of a late Bathonian regressive episode: the Kilmaluag and Skudiburgh Formations of the Great Estuarine Group, Inner Hebrides, Scotland. *J. Geol. Soc. London* **142**, 1119–1137 (1985).
40. J. B. Riding, W. Walton, D. Shaw, Toarcian to Bathonian (Jurassic) palynology of the Inner Hebrides, Northwest Scotland. *Palynology* **15**, 115–179 (1991).
41. J. S. Anderson, R. R. Reisz, D. Scott, N. B. Fröbisch, S. S. Sumida, A stem batrachian from the Early Permian of Texas and the origin of frogs and salamanders. *Nature* **453**, 515–518 (2008).
42. R. R. Schoch, Evolution of life cycles in early amphibians. *Annu. Rev. Earth Planet. Sci.* **37**, 135–162 (2009).
43. R. R. Schoch, Skeleton formation in the Branchiosauridae: A case study in comparing ontogenetic trajectories. *J. Vertebr. Paleontol.* **24**, 309–319 (2004).
44. R. R. Schoch, The putative lissamphibian stem-group: Phylogeny and evolution of the dissorophoid temnospondyls. *J. Paleontol.* **93**, 137–156 (2019).
45. D. Marjanović, M. Laurin, Phylogeny of Paleozoic limbed vertebrates reassessed through revision and expansion of the largest published relevant data matrix. *PeerJ* **6**, e5565 (2019).
46. T. Sigurdsen, J. R. Bolt, The Lower Permian amphibamid *Doleserpeton* (Temnospondyli: Dissorophoidea), the interrelationships of amphibamids, and the origin of modern amphibians. *J. Vertebr. Paleontol.* **30**, 1360–1377 (2010).
47. R. R. Schoch, P. Pogoda, A. Kupfer, The impact of metamorphosis on the cranial osteology of giant salamanders of the genus *Dicamptodon*. *Acta Zool.* **102**, 88–104 (2021).
48. J. Reiss, Palatal metamorphosis in basal caecilians (Amphibia: Gymnophiona) as evidence for lissamphibian monophyly. *J. Herpetol.* **30**, 27–39 (1996).
49. R. R. Schoch, B. S. Rubidge, The amphibamid *Micropholis* from the Lystrosaurus Assemblage Zone of South Africa. *J. Vertebr. Paleontol.* **25**, 502–522 (2005).
50. T. Sigurdsen, The otic region of *Doleserpeton* (Temnospondyli) and its implications for the evolutionary origin of frogs. *Zool. J. Linn. Soc.* **154**, 738–751 (2008).
51. F. A. Jenkins, D. M. Walsh, R. L. Carroll, Anatomy of *Eocaecilia micropodia*, a limbed caecilian of the Early Jurassic. *Bull. Mus. Comp. Zool.* **158**, 285–365 (2007).
52. Y. Rong, Restudy of *Regalerpeton weichangensis* (Amphibia: Urodela) from the Lower Cretaceous of Hebei, China. *Vertebr. Palasiat.* **56**, 121–136 (2018).
53. J. Wiens, R. Bonett, P. Chippindale, Ontogeny discombobulates phylogeny: paedomorphosis and higher-level salamander relationships. *Syst. Biol.* **54**, 91–110 (2005).
54. Z. Szentesi, K. Sebe, M. Szabó, Giant salamander from the Miocene of the Mecsek mountains (Pécs-Danitzpuszta, southwestern Hungary). *PalZ* **94**, 353–366 (2020).
55. R. A. Pyron, J. J. Wiens, A large-scale phylogeny of Amphibia including over 2800 species, and a revised classification of extant frogs, salamanders, and caecilians. *Mol. Phylogenet. Evol.* **61**, 543–583 (2011).
56. J. D. Daza *et al.*, Enigmatic amphibians in mid-Cretaceous amber were chameleon-like ballistic feeders. *Science* **370**, 687–691 (2020).
57. V. de Buffrénil, A. Canoville, S. E. Evans, M. Laurin, Histological study of karaurids, the oldest known (stem) urodeles. *Hist. Biol.* **27**, 109–114 (2015).
58. M. Denoël, P. Joly, H. H. Whiteman, Evolutionary ecology of facultative paedomorphosis in newts and salamanders. *Biol. Rev. Camb. Philos. Soc.* **80**, 663–671 (2005).
59. A. R. Milner, A small temnospondyl amphibian from the Middle Pennsylvanian of Illinois. *Palaeontology* **25**, 635–664 (1982).
60. F. Witzmann, H. Scholz, J. Müller, N. Kardjilov, Sculpture and vascularization of dermal bones, and the implications for the physiology of basal tetrapods. *Zool. J. Linn. Soc.* **160**, 302–340 (2010).
61. M. S. Y. Lee *et al.*, Aquatic adaptations in the four limbs of the snake-like reptile *Tetrapodophis* from the Lower Cretaceous of Brazil. *Cretac. Res.* **66**, 194–199 (2016).
62. J. L. Molnar, Variation in articular cartilage thickness among extant salamanders and implications for limb function in stem tetrapods. *Front. Ecol. Evol.* **9** (2021).
63. J. Fortuny *et al.*, 3D bite modeling and feeding mechanics of the largest living amphibian, the Chinese giant salamander *Andrias davidianus* (Amphibia:Urodela). *PLoS One* **10**, e0121885 (2015).
64. Y. Wang, S. E. Evans, A new short-bodied salamander from the Upper Jurassic-Lower Cretaceous of China. *Acta Palaeontol. Pol.* **51**, 127–130 (2006).
65. S. E. Evans, A. R. Milner, A metamorphosed salamander from the early Cretaceous of Las Hoyas, Spain. *Philos. Trans. R. Soc. Lond. B Biol. Sci.* **351**, 627–646 (1996).
66. J. Jia, K.-Q. Gao, A new hynobiid-like salamander (Amphibia, Urodela) from Inner Mongolia, China, provides a rare case study of developmental features in an Early Cretaceous fossil urodele. *PeerJ* **4**, e2499 (2016).
67. R. R. Schoch, N. B. Fröbisch, Metamorphosis and neoteny: alternative pathways in an extinct amphibian clade. *Evolution* **60**, 1467–1475 (2006).
68. R. M. Bonett, A. L. Trujano-Alvarez, M. J. Williams, E. K. Timpe, Biogeography and body size shuffling of aquatic salamander communities on a shifting refuge. *Proc. Biol. Sci.* **280**, 20130200 (2013).
69. R. A. Pyron, Divergence time estimation using fossils as terminal taxa and the origins of Lissamphibia. *Syst. Biol.* **60**, 466–481 (2011).
70. D. Marjanović, M. Laurin, An updated paleontological timetree of lissamphibians, with comments on the anatomy of Jurassic crown-group salamanders (Urodela). *Hist. Biol.* **26**, 535–550 (2014).
71. S. Mahony, N. M. Foley, S. D. Biju, E. C. Teeling, Evolutionary history of the Asian horned frogs (Megophryinae): integrative approaches to timetree dating in the absence of a fossil record. *Mol. Biol. Evol.* **34**, 744–771 (2017).
72. D. San Mauro, M. Vences, M. Alcobendas, R. Zardoya, A. Meyer, Initial diversification of living amphibians predated the breakup of Pangaea. *Am. Nat.* **165**, 590–599 (2005).
73. F. Bossuyt, R. M. Brown, D. M. Hillis, D. C. Cannatella, M. C. Milinkovitch, Phylogeny and biogeography of a cosmopolitan frog radiation: Late Cretaceous diversification resulted in continent-scale endemism in the family ranidae. *Syst. Biol.* **55**, 579–594 (2006).
74. P. Zhang, D. B. Wake, Higher-level salamander relationships and divergence dates inferred from complete mitochondrial genomes. *Mol. Phylogenet. Evol.* **53**, 492–508 (2009).
75. M.-Y. Chen *et al.*, A reinvestigation of phylogeny and divergence times of Hynobiidae (Amphibia, Caudata) based on 29 nuclear genes. *Mol. Phylogenet. Evol.* **83**, 1–6 (2015).
76. X.-X. Shen *et al.*, Enlarged multilocus data set provides surprisingly younger time of origin for the Plethodontidae, the largest family of salamanders. *Syst. Biol.* **65**, 66–81 (2016).
77. I. Irisarri *et al.*, Phylotranscriptomic consolidation of the jawed vertebrate timetree. *Nat. Ecol. Evol.* **1**, 1370–1378 (2017).
78. Y.-J. Feng *et al.*, Phylogenomics reveals rapid, simultaneous diversification of three major clades of Gondwanan frogs at the Cretaceous-Paleogene boundary. *Proc. Natl. Acad. Sci. U.S.A.* **114**, E5864–E5870 (2017).
79. P. M. Hime *et al.*, Phylogenomics reveals ancient gene tree discordance in the amphibian tree of life. *Syst. Biol.* **70**, 49–66 (2021).
80. K. Roelants *et al.*, Global patterns of diversification in the history of modern amphibians. *Proc. Natl. Acad. Sci. U.S.A.* **104**, 887–892 (2007).
81. Y. Zheng, R. Peng, M. Kuro-o, X. Zeng, Exploring patterns and extent of bias in estimating divergence time from mitochondrial DNA sequence data in a particular lineage: a case study of salamanders (order Caudata). *Mol. Biol. Evol.* **28**, 2521–2535 (2011).
82. B. G. Naylor, Cryptobranchid salamanders from the Paleocene and Miocene of Saskatchewan. *Copeia* **1981**, 76–86 (1981).
83. D. Vasilyan, M. Böhme, Pronounced peramorphosis in lissamphibians–*Aviturus exsecratus* (Urodela, Cryptobranchidae) from the Paleocene-Eocene Thermal Maximum of Mongolia. *PLoS One* **7**, e40665 (2012).
84. D. San Mauro, A multilocus timescale for the origin of extant amphibians. *Mol. Phylogenet. Evol.* **56**, 554–561 (2010).

Downloaded from https://www.pnas.org by UCL Library Services on July 25, 2022 from IP address 128.41.35.168.

85. J. D. Gardner, Revision of *Habrosaurus* Gilmore (Caudata; Sirenidae) and relationships among sirenid salamanders. *Palaeontology* **46**, 1089–1122 (2003).
86. J. D. Gardner, The fossil salamander *Proamphiuma cretacea* Estes (Caudata; Amphiumidae) and relationships within the Amphiumidae. *J. Vertebr. Paleontol.* **23**, 769–782 (2003).
87. S. E. Evans, D. Sigogneau-Russell, A stem-group caecilian (Lissamphibia: Gymnophiona) from the Lower Cretaceous of North Africa. *Palaeontology* **44**, 259–273 (2001).
88. C. Sullivan *et al.*, The vertebrates of the Jurassic Daohugou Biota of northeastern China. *J. Vertebr. Paleontol.* **34**, 243–280 (2014).
89. S. Smirnov, Extra bones in the *Pelobates* skull as evidence of the paedomorphic origin in the anurans. *Zhurnal Obshcheĭ Biol.* **56**, 317–328 (1995).
90. R. R. Schoch, Amphibian skull evolution: the developmental and functional context of simplification, bone loss and heterotopy. *J. Exp. Zoolog. B Mol. Dev. Evol.* **322**, 619–630 (2014).
91. M. I. Coates, J. A. Clack, Fish-like gills and breathing in the earliest known tetrapod. *Nature* **352**, 234–236 (1991).
92. T. L. Kivell, J. M. Kibii, S. E. Churchill, P. Schmid, L. R. Berger, *Australopithecus sediba* hand demonstrates mosaic evolution of locomotor and manipulative abilities. *Science* **333**, 1411–1417 (2011).
93. Z. Zhou, F. Zhang, Largest bird from the Early Cretaceous and its implications for the earliest avian ecological diversification. *Naturwissenschaften* **89**, 34–38 (2002).
94. T. Imai *et al.*, An unusual bird (Theropoda, Avialae) from the Early Cretaceous of Japan suggests complex evolutionary history of basal birds. *Commun. Biol.* **2**, 399 (2019).
95. M. E. H. Jones *et al.*, Salamander morphology, morphosource, https://www.morphosource.org/projects/00000C868. Deposited 3 October 2019.
96. F. Ronquist *et al.*, MrBayes 3.2: Efficient Bayesian phylogenetic inference and model choice across a large model space. *Syst. Biol.* **61**, 539–542 (2012).
97. T. A. Heath, J. P. Huelsenbeck, T. Stadler, The fossilized birth-death process for coherent calibration of divergence-time estimates. *Proc. Natl. Acad. Sci. U.S.A.* **111**, E2957–E2966 (2014).
98. M. E. H. Jones *et al.*, Middle Jurassic fossils document an early stage in salamander evolution. Open Science Framework. 10.17605/OSF.IO/QAXDF. Deposited 30 November 2021.
99. D. Swofford, *PAUP* Phylogenetic Analysis Using Parsimony v. 4.0a151* (Sinauer Associates).

Downloaded from https://www.pnas.org by UCL Library Services on July 25, 2022 from IP address 128.41.35.168.